RESEARCH PAPERS

Acta Cryst. (1999). B**55**, 830–840

Charge density in $NiCl_2.4H_2O$ at 295 and 30 K

H. Ptasiewicz-Bak,[a]† I. Olovsson[a]* and G. J. McIntyre[b]

[a]*Inorganic Chemistry, Ångström Laboratory, University of Uppsala, Box 538, S-751 21 Uppsala, Sweden, and* [b]*Institut Laue-Langevin, BP 156, 38042 Grenoble CEDEX 9, France. E-mail: ivar.olovsson@kemi.uu.se*

(*Received 25 November 1998; accepted 23 April 1999*)

Abstract

The charge distribution has been determined by multipole refinements against single-crystal X-ray diffraction data. In the refinements a comparison was made between the densities based on H-atom parameters from X-ray and neutron data, respectively. X-ray study: λ(Mo $K\alpha$) = 0.71073 Å, $F(000)$ = 408; at 30 K: $R(F)$ = 0.015 for 6686 reflections; at 295 K: $R(F)$ = 0.022 for 4630 reflections. The nickel ion is octahedrally surrounded by four water molecules and two chloride ions, forming a locally neutral $Ni(H_2O)_4Cl_2$ complex. Two of the water molecules are coordinated to nickel approximately in one of the tetrahedral ('lone-pair') directions; the other two are trigonally coordinated. At 30 K one H atom in one of the trigonally coordinated water molecules is disordered, with equal occupation of two different positions. Owing to the polarizing influence of the nickel ion there are two peaks in the lone-pair plane of the water molecules when these are tetrahedrally coordinated; for those trigonally coordinated there is just one peak. The individual ('partial') charge densities, calculated from the deformation functions of only nickel or the separate water molecules, have also been calculated to study the effects of superposition of the individual densities. In the individual density of nickel an excess is observed in the diagonal directions and a deficiency in the ligand directions. However, owing to the influence of the whole crystalline environment, the maxima around nickel are not found in the planes defined by nickel and the six ligands.

1. Introduction

The present investigation is part of a series of studies on the charge density in hydrates of transition-metal salts. Earlier works in this series include $NiSO_4.6H_2O$ (McIntyre *et al.*, 1990; Ptasiewicz-Bak *et al.*, 1993), $NiSO_4.7H_2O$ (Ptasiewicz-Bak *et al.*, 1997), $Na_2Ni(CN)_4.3H_2O$ (Ptasiewicz-Bak *et al.*, 1998) and $CoSO_4.6H_2O$ (Kellersohn *et al.*, 1993). The details of the charge density of the metal ions as well as the influence of the environment on the charge density of the water molecules have been studied in model deformation density maps. In these studies it was demonstrated that the true bonding features are often obscured in maps based on the complete structure by superposition of the densities of adjacent atoms/molecules. The use of *partial* model deformation maps, calculated only from the deformation functions centred on the individual atoms or molecules, appears to be an effective way of overcoming these superposition effects and the resulting maps appear physically sensible (*cf.* Olovsson *et al.*, 1993). For example, the partial maps show clear polarization of the lone-pair densities of the water O atoms according to the coordination, tetrahedral or planar trigonal, of the water molecules. In $NiCl_2.4H_2O$ there are four crystallographically independent water molecules with rather different bonding situations, which offers a good opportunity to study the effects of the different local environments on the charge density of water.

2. Experimental

Light-green translucent crystals of $NiCl_2.4H_2O$ were grown from an aqueous solution of $NiCl_2$ at 323 K.

2.1. *Neutron data*

Despite many attempts it was not possible to obtain a crystal of good quality with sufficient volume for neutron diffraction. The crystal finally selected for the neutron data collection contained several crystallites with almost coincident orientation. Data were measured from this crystal at 295 K and 30 K on the D9 four-circle diffractometer at the Institut Laue-Langevin, Grenoble, in a beam of wavelength 0.8405 (2) Å obtained by reflection from a Cu(220) monochromator. This diffractometer is equipped with a small two-dimensional area detector (Lehmann *et al.*, 1989), which for this measurement allowed reasonably optimal delineation of Bragg reflections from the considerable incoherent background of hydrogen despite the presence of several peaks. Almost complete sets of unique reflections out to $\sin\theta/\lambda = 0.7647$ Å^{-1} were scanned; ω–$x\theta$ step scans, with x increasing from 1.0 at low θ to 1.7 at the highest θ. One

† Permanent address: Institute of Nuclear Chemistry and Technology, Dorodna 16, 03-195 Warsaw, Poland.

standard reflection measured at regular intervals showed no significant variation with time. Background corrections following Wilkinson *et al.* (1988), with allowance for the contribution by several peaks to each reflection, and Lorentz corrections were applied; correction was also applied for absorption in the cylindrical cryostat heat shields, transmission range 0.9669–0.9743. Other experimental details are given in Table 1.

2.2. *X-ray data*

Intensity data were collected at 295 K and 30 K. The four-circle diffractometer was equipped with a two-stage closed-cycle helium refrigerator (Samson *et al.*, 1980). Graphite(002)-monochromated Mo $K\alpha$ radiation was used in both measurements. Reflections were measured up to $\sin\theta/\lambda = 1.09$ Å^{-1} at 295 K and to $\sin\theta/\lambda = 1.12$ Å^{-1} at 30 K. The average instability constant was 0.018 at 295 K and 0.005 at 30 K. Background corrections followed Lehmann & Larsen (1974) and standard deviations were estimated from counting statistics; Lorentz and polarization corrections were applied. Other experimental details are given in Table 1.

All data-reduction programs and the full-matrix least-squares program *UPALS* used for structure refinement have been described by Lundgren (1982).

3. Refinements

The crystal structure of the title compound was previously studied by Stroganov *et al.* (1960). However, the space group was incorrectly reported as tetragonal and the structure as composed of $[Ni(H_2O)_6]_2NiCl_6$.

The structure was later correctly determined by Waizumi *et al.* (1992) in the space group $P2_1/a$ with $\beta = 126.45\ (1)^\circ$. However, the unit-cell axes can be chosen with β closer to 90° [$\beta = 100.32\ (3)^\circ$] in the alternative space group $P2_1/n$. We solved the structure independently from Patterson maps based on our X-ray data in $P2_1/n$. The asymmetric unit contains one Ni atom, two Cl atoms and four water molecules.

3.1. *Neutron data*

Refinement details are given in Table 1. The scattering lengths for Ni, Cl, O and H were 1.0300, 0.9578, 0.5803 and -0.3741×10^{-12} cm, respectively, taken from Sears (1986). The starting models for the neutron refinements at both temperatures were from the conventional X-ray refinement (see below) with no disorder for any of the atoms.

The parameters for H42 initially refined to rather abnormal values, *e.g.* with O4—H42 0.79 Å (where O4 is the O atom in the same water molecule as H42) and an isotropic parameter $U_{eq} = 0.15$ Å^2 at 30 K. These results might be blamed on the poor quality of the crystal used in the neutron diffraction experiment. However, comparison with the results from the conventional X-ray refinement indicated that there were real structural reasons for the abnormal results. First, the average discrepancy between the atomic coordinates for non-H atoms from the neutron and X-ray deformation refinements is 1.6σ(neutrons), which indicates that the neutron values are reliable. Secondly, U_{eq} for H42 was larger at 30 K than at 295 K, and the ratio between U_{eq} for H42 and the average U_{eq} for the other H atoms was ~5 at 30 K and ~2 at 295 K, both from X-rays and neutrons. Close inspection of the residual maps after the conventional X-ray refinement at 30 K, excluding atom H42 in the difference calculation, revealed two peaks; two peaks were not found at 295 K. There were no comparable peaks around the other H atoms at either temperatures. Allowing for the possibility of disorder in H42 in the neutron refinements resulted in two sites, H421 and H422, 0.93 (4) Å apart with occupancies of 0.52 (5) and 0.48 (5), respectively, and with U_{eq} values very similar to those for the other H atoms. Refinement of these two H-atom positions, based on the neutron data at 295 K, resulted in an occupancy of 1.0 for the first position and 0.0 for the other. Evidently there is no disorder for H42 at 295 K. As expected, the refined position of H42 at 30 K (see above) is the average of the two positions for H421 and H422. Atomic coordinates and equivalent isotropic displacement parameters following the final neutron refinements are given in Table 2.†

Although the *R*-factors and least-squares goodness of fit were large at both temperatures because of the poor data quality, the precision in the resulting coordinates was nevertheless acceptable and the neutron coordinates for hydrogen could be used in the deformation refinements. Independently, H-atom coordinates determined by X-rays were also used in the deformation refinements.

3.2. *X-ray data*

Two sets of refinement were carried out for both the 295 K and 30 K data: (i) a conventional refinement with the assumption of spherical atomic scattering factors, and (ii) deformation refinements in which the experimental electron distribution was fitted to multipole deformation functions. In the weighting scheme k was fixed at 0.01. The constant k was determined from analyses of the weighted $F_o^2 - F_c^2$ as functions of intensity and $\sin\theta$ for different values of k.

For both the 295 K and 30 K data the positional parameters for hydrogen were fixed to the neutron values. The refined coordinates for atoms other than H agreed well with the neutron coordinates, but the displacement parameters were systematically larger in

† Supplementary data for this paper are available from the IUCr electronic archives (Reference: OS0021). Services for accessing these data are described at the back of the journal.

Table 1. *Experimental details*

	295 K, X-ray	295 K, neutron	30 K, X-ray	30 K, neutron
Paul Crystal data				
Chemical formula	$Cl_2Ni.4(H_2O)$	$Cl_2Ni.4(H_2O)$	$Cl_2Ni.4(H_2O)$	$Cl_2Ni.4(H_2O)$
Chemical formula weight	201.7	201.7	201.7	201.7
Cell setting	Monoclinic	Monoclinic	Monoclinic	Monoclinic
Space group	$P2_1/n$	$P2_1/n$	$P2_1/n$	$P2_1/n$
a (Å)	5.985 (3)	6.006 (3)	5.961 (3)	5.968 (2)
b (Å)	9.291 (5)	9.338 (5)	9.273 (5)	9.283 (3)
c (Å)	10.931 (6)	10.986 (5)	10.891 (7)	10.897 (3)
β (°)	100.32 (3)	100.45 (3)	100.02 (5)	100.08 (2)
V (Å^3)	598 (1)	606 (1)	593 (1)	594 (1)
Z	4	4	4	4
D_x (Mg m^{-3})	2.240	2.211	2.260	2.254
Radiation type	Mo $K\alpha$	Neutron	Mo $K\alpha$	Neutron
Wavelength (Å)	0.71073	0.8405	0.71073	0.8405
No. of reflections for cell parameters	20	175	20	233
θ range (°)	15–25	3–40	15–25	3–40
μ (mm^{-1})	4.05	0.236	4.09	0.239
Temperature (K)	295 (2)	295 (2)	30 (1)	30 (1)
Crystal form	Trapezoidal pyramid with 20 faces	Trapezoidal pyramid with 20 faces	Trapezoidal pyramid with 20 faces	Trapezoidal pyramid with 20 faces
Crystal size (mm)	0.23 × 0.20 × 0.09	4.0 × 2.0 × 1.7	0.21 × 0.20 × 0.08	4.0 × 2.0 × 1.7
Crystal colour	Light green	Light green	Light green	Light green
Data collection				
Diffractometer	Stoe four-circle	D9 four-circle	Stoe four-circle	D9 four-circle
Data collection method	ω–2θ scans	ω–$x\theta$ scans	ω–2θ scans	ω–$x\theta$ scans
Absorption correction	Gaussian	Gaussian	Gaussian	Gaussian
T_{min}	0.4806	0.6439	0.4304	0.6806
T_{max}	0.5644	0.7383	0.6348	0.7481
No. of measured reflections	6710	2292	7534	1566
No. of independent reflections	6137	2292	6686	1566
No. of observed reflections	4630	2237	6686	1503
Criterion for observed reflections	$F_o^2 > 3\sigma(F_o^2)$	Unaffected by parasite peaks	$F_o^2 > 3\sigma(F_o^2)$	Unaffected by parasite peaks
R_{int}	0.024	0	0.019	0
θ_{max} (°)	50.8	40	52.6	40
Range of h, k, l	$-6 \rightarrow h \rightarrow 13$ $0 \rightarrow k \rightarrow 20$ $-23 \rightarrow l \rightarrow 23$	$0 \rightarrow h \rightarrow 9$ $0 \rightarrow k \rightarrow 14$ $-16 \rightarrow l \rightarrow 16$	$-13 \rightarrow h \rightarrow 13$ $-20 \rightarrow k \rightarrow 20$ $-5 \rightarrow l \rightarrow 24$	$0 \rightarrow h \rightarrow 9$ $0 \rightarrow k \rightarrow 14$ $-16 \rightarrow l \rightarrow 16$
No. of standard reflections	6	1	6	1
Frequency of standard reflections	Every 240 min	Every 120 min	Every 240 min	Every 120 min
Refinement				
Refinement on	F^2	F^2	F^2	F^2
$R[F^2>2\sigma(F^2)]$	0.0284	0.18	0.0215	0.126
$wR(F^2)$	0.0341	0.17	0.0327	0.142
S	1.312	2.34	1.421	2.99
No. of reflections used in refinement	4630	2237	6686	1503
No. of parameters used	164	136	164	136
H-atom treatment	H atoms: placed at positions found by neutron diffraction, see text	H atoms refined	H atoms: placed at positions found by neutron diffraction, see text	H atoms refined
Weighting scheme	$w = 1/[\sigma^2(F_o^2) + k^2F_o^4]$	$w = 1/[\sigma^2(F_o^2) + k^2F_o^4]$	$w = 1/[\sigma^2(F_o^2) + k^2F_o^4]$	$w = 1/[\sigma^2(F_o^2) + k^2F_o^4]$
$(\Delta/\sigma)_{max}$	0.005	0.03	0.006	0.03
$\Delta\rho_{max}$ (e Å^{-3})	0.15	0	0.15	0
$\Delta\rho_{min}$ (e Å^{-3})	−0.15	0	−0.15	0
Extinction method	Gaussian type I isotropic (Becker & Coppens, 1974, 1975)	No correction	Gaussian type I isotropic (Becker & Coppens, 1974, 1975)	No correction
Extinction coefficient	49 200	0	1110	0

Table 1 (*cont.*)

	295 K, X-ray	295 K, neutron	30 K, X-ray	30 K, neutron
Source of atomic scattering factors	*International Tables for X-ray Crystallography* (1974, Vol. IV) for Ni, Cl, and O, and Stewart *et al.* (1965) for H	Sears (1986)	*International Tables for X-ray Crystallography* (1974, Vol. IV) for Ni, Cl, and O, and Stewart *et al.* (1965) for H	Sears (1986)
Computer programs				
Data collection	Stoe four-circle Diffractometer Control Program	Diffractometer Control Program D9	Stoe four-circle Diffractometer Control Program	Diffractometer Control Program D9
Cell refinement	Stoe four-circle Diffractometer Control Program	Diffractometer Control Program D9	Stoe four-circle Diffractometer Control Program	Diffractometer Control Program D9
Data reduction	*DATRED* (Lundgren, 1982)	Wilkinson *et al.* (1988)	*DATRED* (Lundgren, 1982)	Wilkinson *et al.* (1988)
Structure refinement	*UPALS* (Lundgren, 1982)	*UPALS* (Lundgren, 1982)	*UPALS* (Lundgren, 1982)	*UPALS* (Lundgren, 1982)

the neutron case. The average ratio β(X-ray)/β(neutron) for atoms other than H was 0.80 for both temperatures, with little individual variation. In the final X-ray refinements the anisotropic displacement parameters for hydrogen were therefore fixed to the neutron values multiplied by 0.80. It may be remarked that in the literature the ratio β(X-ray)/β(neutron) has sometimes been found to be greater than 1 and sometimes less than 1. For example, in $NiSO_4.7H_2O$ at 25 K the ratio was found to be 0.872 (Ptasiewicz-Bak *et al.*, 1997), but in $NiSO_4.6D_2O$ at 295 K the ratio was 1.38 (McIntyre *et al.*, 1990). The differences in the ratio may be due to differences in the amount of included thermal-diffuse scattering arising from the different integration volumes in the different X-ray and neutron experiments.

In the charge-density determination we also compared the maps based on parameters for hydrogen determined by neutron diffraction with maps from refinements based on positional and isotropic displacement parameters for hydrogen from the X-ray conventional refinement, but with the hydrogen positions shifted out to 0.97 Å along the O—H bond.

3.2.1. *Conventional refinement*. The following parameters were refined: scale factor, mosaic width, positional and anisotropic displacement parameters of all atoms other than the H atoms; the positional and isotropic displacement parameters for H atoms were also refined. At 295 K, $R(F)$ = 0.023, $R(F^2)$ = 0.033, $wR(F^2)$ = 0.039, S = 1.69; at 30 K, the corresponding values were 0.017, 0.024, 0.038 and 1.63, respectively. The residual maps have been discussed above (see §3.1).

3.2.2. *Deformation refinement*. The experimental deformation density was modelled by multipole refinement by least squares, using deformation functions

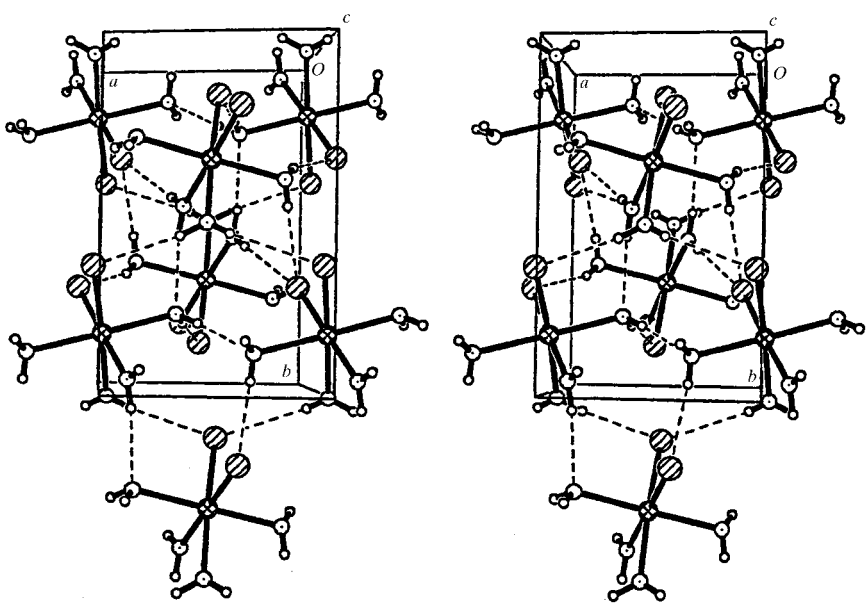

Fig. 1. Stereoscopic picture of the crystal structure of $NiCl_2.4H_2O$ at 295 K. The *c*-axis is directed towards the reader.

Table 2. *Fractional atomic coordinates and equivalent isotropic displacement parameters (Å²)*

(*a*) $NiCl_2.4H_2O$ at 295 K from X-ray multipole refinement. H from neutrons (see text). (*b*) $NiCl_2.4H_2O$ at 295 K from neutron refinement. (*c*) $NiCl_2.4H_2O$ at 30 K from X-ray multipole refinement. H from neutrons (see text). (*d*) $NiCl_2.4H_2O$ at 30 K from neutron refinement. For H421 and H422, occupancy of 0.52 (5) and 0.48 (5), respectively.

	x	*y*	*z*	U_{eq}
(*a*)				
Ni	0.01357 (2)	0.16902 (1)	0.26396 (1)	0.0144 (1)
Cl1	−0.02924 (2)	0.36300 (2)	0.12066 (1)	0.0207 (1)
Cl2	0.09642 (2)	0.69421 (2)	0.57077 (1)	0.0227 (1)
O1	0.34593 (11)	0.22553 (6)	0.33707 (5)	0.0208 (2)
O2	−0.32321 (8)	0.11558 (6)	0.19534 (7)	0.0202 (3)
O3	0.12495 (11)	0.04131 (7)	0.13162 (6)	0.0286 (4)
O4	0.03767 (9)	−0.01607 (9)	0.36810 (6)	0.0283 (3)
(*b*)				
Ni	0.0139 (3)	0.1694 (2)	0.2639 (2)	0.019 (1)
Cl1	−0.0288 (4)	0.3625 (2)	0.1208 (2)	0.024 (1)
Cl2	−0.0949 (4)	0.6947 (2)	0.5708 (2)	0.028 (1)
O1	0.3513 (7)	0.2252 (4)	0.3366 (4)	0.026 (2)
O2	−0.3244 (7)	0.1164 (4)	0.1953 (4)	0.026 (2)
O3	0.1225 (8)	0.0419 (5)	0.1315 (4)	0.035 (2)
O4	0.0358 (8)	−0.0174 (5)	0.3672 (4)	0.033 (2)
H11	0.387 (2)	0.194 (1)	0.423 (1)	0.050 (4)
H12	0.454 (2)	0.192 (1)	0.299 (1)	0.051 (5)
H21	−0.360 (1)	0.152 (1)	0.113 (1)	0.056 (5)
H22	−0.346 (1)	0.014 (1)	0.187 (1)	0.053 (5)
H31	0.192 (1)	0.076 (1)	0.067 (1)	0.057 (5)
H32	0.159 (2)	−0.058 (1)	0.146 (1)	0.051 (5)
H41	0.178 (2)	−0.064 (1)	0.388 (1)	0.053 (5)
H42	−0.086 (3)	−0.057 (1)	0.393 (1)	0.112 (11)
(*c*)				
Ni	0.01461 (1)	0.16986 (1)	0.26586 (1)	0.00333 (2)
Cl1	−0.02658 (2)	0.36338 (1)	0.12080 (1)	0.00779 (4)
Cl2	0.09570 (2)	0.68988 (1)	0.56924 (1)	0.00556 (4)
O1	0.34847 (7)	0.22745 (4)	0.33802 (3)	0.0067 (1)
O2	−0.32509 (6)	0.11736 (4)	0.19799 (4)	0.0070 (1)
O3	0.12182 (7)	0.03982 (4)	0.13301 (4)	0.0084 (1)
O4	0.03855 (6)	−0.01465 (5)	0.37314 (4)	0.0097 (1)
(*d*)				
Ni	0.0144 (4)	0.1700 (2)	0.2660 (2)	0.005 (1)
Cl1	−0.0260 (4)	0.3635 (2)	0.1209 (2)	0.009 (1)
Cl2	−0.0948 (4)	0.6899 (2)	0.5688 (2)	0.007 (1)
O1	0.3499 (7)	0.2281 (4)	0.3385 (3)	0.008 (2)
O2	−0.3263 (7)	0.1170 (4)	0.1987 (3)	0.009 (2)
O3	0.1210 (7)	0.0400 (4)	0.1333 (3)	0.008 (2)
O4	0.0405 (10)	−0.0164 (4)	0.3739 (3)	0.011 (2)
H11	0.399 (1)	0.199 (1)	0.426 (1)	0.028 (4)
H12	0.468 (1)	0.188 (1)	0.296 (1)	0.019 (3)
H21	−0.375 (2)	0.154 (1)	0.114 (1)	0.038 (5)
H22	−0.352 (2)	0.014 (1)	0.187 (1)	0.036 (4)
H31	0.192 (2)	0.076 (1)	0.064 (1)	0.032 (4)
H32	0.153 (2)	−0.062 (1)	0.143 (1)	0.032 (4)
H41	0.175 (2)	−0.065 (1)	0.383 (1)	0.035 (5)
H421	−0.097 (4)	−0.070 (2)	0.376 (2)	0.037 (13)
H422	−0.019 (4)	−0.021 (2)	0.446 (2)	0.027 (12)

proposed by Hirshfeld (1971) with modifications by Harel & Hirshfeld (1975) and Hirshfeld (1977). The charge density was modelled by an expansion of up to 35 terms centred on each atom. Details of the procedure have been given in a previous paper (McIntyre *et al.*, 1990).

A series of deformation refinements were performed where initially imposed symmetry constraints were successively relaxed and the level of multipoles n increased. Strong correlation effects prohibited simultaneous refinement of the γ parameters, which determine the breadth of the radial functions, together with the other deformation functions. Therefore, their values were chosen on the basis of an analysis of the results of refinements with fixed γ parameters in the range γ = 3.5–6 for nickel and in the range γ = 2.5–3.5 for the other atoms. Gaussian radial functions were used, since for exponential radial functions the refinements diverged. Modifying the values of γ within reasonable limits had very little effect on the total deformation density maps, but γ values outside these limits changed the maps drastically and were not chemically reasonable. In the final refinements γ for Ni was fixed to 5.0, and for all other atoms to 3.0. In the final refinements at both temperatures the following parameters were varied:

(*a*) Ni: x, y, z, β_{ij}; $n \leq 4$; 31 deformation parameters.

(*b*) O: x, y, z, β_{ij}; $n \leq 4$; 14 deformation parameters per atom; *mm*2 symmetry imposed within each water molecule. All O atoms treated independently.

(*c*) Cl: x, y, z, β_{ij}; $n \leq 2$; four deformation parameters per atom; cylindrical symmetry imposed about each Ni—Cl bond. The two Cl atoms treated independently.

(*d*) H: $n \leq 2$; four deformation parameters; cylindrical symmetry imposed about each O—H bond. All H atoms assumed to be equivalent. The positional and displacement parameters were fixed as described above.

A total of 99 deformation parameters were refined. In addition, the scale factor, an isotropic extinction parameter, and the position and thermal-displacement parameters of all atoms other than H were refined. The root-mean-square mosaic spread was 1.2 s at 295 K and 52.6 s at 30 K.

Positional and equivalent isotropic displacement parameters from the final model deformation refinements are given in Table 2. Selected bond lengths and angles are given in Table 3.

4. Results and discussion

A stereoscopic picture of the structure at 295 K is shown in Fig. 1. The nickel ion is octahedrally surrounded by four water molecules and two chloride ions, forming a locally neutral $Ni(H_2O)_4Cl_2$ complex (Fig. 2). The average Ni—O distance is 2.075 (1) Å at 30 K and 2.070 (1) Å at 295 K (without correction for thermal motion, which explains the shorter distances at 295 K). The corresponding average values in our earlier-studied Ni compounds are 2.052 (1) and 2.048 (1) Å, at 30 and 295 K, respectively. The distances at 295 K agree within two estimated standard deviations with the distances

Table 3. *Selected bond lengths (Å) and angles (°) from multipole refinements with H from neutrons (see text) for $NiCl_2.4H_2O$ at 30 (first entry) and 295 K (second entry)*

(*a*) Covalent bonds			
Ni—O1	2.078 (1)	O1—Ni—O2	177.86 (2)
	2.074 (1)		178.18 (3)
Ni—O2	2.089 (1)	O1—Ni—O3	91.27 (4)
	2.081 (1)		90.44 (4)
Ni—O3	2.068 (1)	O1—Ni—O4	91.81 (4)
	2.071 (1)		91.79 (3)
Ni—O4	2.063 (1)	O2—Ni—O3	90.86 (4)
	2.053 (1)		91.36 (4)
Ni—Cl1	2.375 (1)	O2—Ni—O4	88.53 (4)
	2.371 (1)		88.13 (3)
Ni—Cl2	2.400 (1)	O3—Ni—O4	85.03 (5)
	2.395 (1)		84.72 (4)
		Cl1—Ni—Cl2	94.49 (4)
			94.77 (4)
		Cl1—Ni—O4	172.93 (1)
			172.47 (2)
		Cl2—Ni—O3	176.07 (1)
			175.49 (2)
(*b*) Water molecules			
O1—H11	0.992 (7)	H11—O1—H12	103.4 (7)
	0.974 (8)		105.4 (8)
O1—H12	0.985 (8)		
	0.889 (9)		
O2—H21	0.972 (8)	H21—O2—H22	102.6 (8)
	0.951 (9)		104.6 (9)
O2—H22	0.976 (8)		
	0.959 (8)		
O3—H31	0.981 (8)	H31—O3—H32	108.9 (7)
	0.931 (9)		111.1 (8)
O3—H32	0.970 (8)		
	0.957 (9)		
O4—H41	0.933 (12)	H41—O4—H42	–
	0.945 (9)		118.1 (1.1)
O4—H42	–		
	0.921 (17)		
O4—H421	0.963 (23)	H41—O4—H421	116.9 (1.4)
	–		–
O4—H422	0.921 (28)	H41—O4—H422	108.5 (1.5)
	–		–
(*c*) Hydrogen bonds			
D—H···*A*	*D*···*A*	H···*A*	*D*—H···*A*
O1—H11···Cl1^{ii}	3.154 (2)	2.166 (7)	174.1 (8)
	3.165 (2)	2.193 (8)	175.8 (8)
O1—H12···O2^{i}	2.861 (1)	1.881 (7)	173.6 (6)
	2.909 (1)	2.024 (9)	174.1 (8)
O2—H21···Cl2^{iv}	3.145 (2)	2.220 (8)	158.6 (9)
	3.157 (2)	2.272 (9)	154.4 (8)
O2—H22···Cl2^{iii}	3.174 (1)	2.277 (8)	152.5 (8)
	3.184 (1)	2.302 (9)	152.5 (9)
O3—H31···Cl2^{v}	3.304 (2)	2.336 (8)	168.8 (7)
	3.319 (1)	2.398 (9)	170.1 (8)
O3—H32···O1^{iv}	2.916 (2)	1.957 (8)	168.9 (9)
	2.955 (2)	2.016 (9)	166.5 (8)
O4—H41···Cl1^{iv}	3.111 (1)	2.202 (13)	164.7 (8)
	3.131 (2)	2.223 (9)	160.6 (8)
O4—H42···Cl1^{vi}	–	–	–
	3.266 (2)	2.394 (18)	158 (1)
O4—H421···Cl1^{vi}	3.266 (2)	2.332 (29)	163 (2)
	–	–	–
O4—H422···O^{vii}	2.893 (2)	2.022 (29)	157 (2)
	–	–	–

Symmetry codes: (i) $x+1, y, z$; (ii) $x+\frac{1}{2}, -y+\frac{1}{2}, z+\frac{1}{2}$; (iii) $x-\frac{1}{2}, -y+\frac{1}{2}, z-\frac{1}{2}$; (iv) $-x+\frac{1}{2}, y-\frac{1}{2}, -z+\frac{1}{2}$; (v) $-x+\frac{3}{2}, y-\frac{1}{2}, -z+\frac{1}{2}$; (vi) $-x-\frac{1}{2}, y-\frac{1}{2}, -z+\frac{1}{2}$; (vii) $-x, -y, -z+1$.

obtained by Waizumi *et al.* (1992). It is notable that the chloride ions are in a *cis* position relative to each other, and not *trans* as might be expected from a charge-repulsion point of view.

Two of the water molecules are coordinated to nickel approximately in one of the tetrahedral ('lone-pair') directions, the other two are both trigonally coordinated at 295 K (Fig. 3). At 30 K the water (4) molecule with an orientation corresponding to H41—O4—H421 is tetrahedrally coordinated to Ni (β = 25.4 and α = 25.2°) and H422 of the neighbouring complex. The water (4) molecule with an orientation corresponding to H41—O4—H422 is coordinated only to Ni (β = 30.7 and α = 27.3°). All four water molecules donate two hydrogen bonds to water O atoms or chloride ions. At 30 K H421

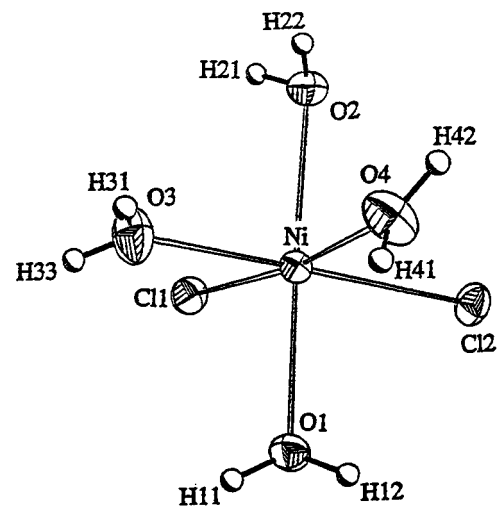

Fig. 2. The approximately octahedral coordination of the six ligands around nickel at 295 K. Thermal ellipsoids correspond to 50% probability.

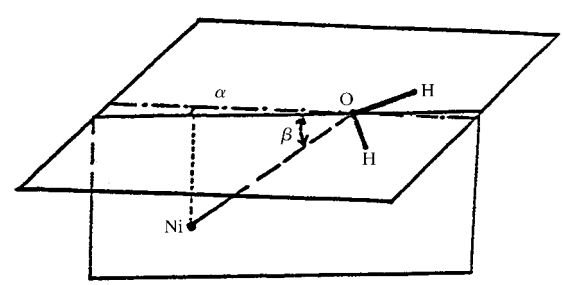

Plane	β (°)	α (°)
(O1,H11,H12)	45.8	2.1
(O2,H21,H22)	52.2	3.8
(O3,H31,H32)	14.2	2.1
(O4,H41,H42)	1.6	8.4

Fig. 3. The geometry of the coordination of the water molecules to nickel at 295 K.

forms a hydrogen bond to Cl1, and H422 to O4 of the neighbouring $Ni(H_2O)_4Cl_2$ complex. H41 is not disordered, as also shown by the similar U_{eq} to other H atoms. At 295 K only the hydrogen bond to Cl1 is formed.

The shortest distance between the H422 sites of neighbouring $Ni(H_2O)_4Cl_2$ complexes is 1.23 (6) Å, which precludes water (4) molecules of the neighbouring complexes, both being in the orientation H41—O—H422. Alternating orientations (O—H421 and O—H422, respectively) in neighbouring complexes are quite acceptable since the distances H41···H421, H41···H422 and H421···H422 are all at least 2.1 Å. This suggests that the structure might have long-range ordering of water (4) to give a symmetry lower than $P2_1/n$. Close inspection of both the X-ray and neutron data showed that the space group $P2_1/n$ is, however, still obeyed at 30 K. The alternate ordering of water (4) in one pair of neighbouring $Ni(H_2O)_4Cl_2$ complexes is thus uncorrelated with the ordering in adjacent pairs.

4.1. *Deformation electron densities*

Some general arguments for the use of deformation model maps instead of *X–N* maps were given in a previous paper (McIntyre *et al.*, 1990). This approach also makes it possible to calculate partial deformation maps that eliminate effects due to superposition of the deformation functions of neighbouring atoms (*cf.* Olovsson *et al.*, 1993).

In the maps the three atoms defining each plane are written without parentheses. For orientation purposes other atoms close to these planes, and the relevant H atoms, are indicated within parentheses. In an attempt to distinguish the characteristic features of the nickel ion and the water molecules, the partial maps calculated from only the deformation functions of each of these constituents are also plotted separately. All maps shown are static multipole deformation maps; the corresponding dynamic maps are very similar. Only a few of all the maps calculated are illustrated here.

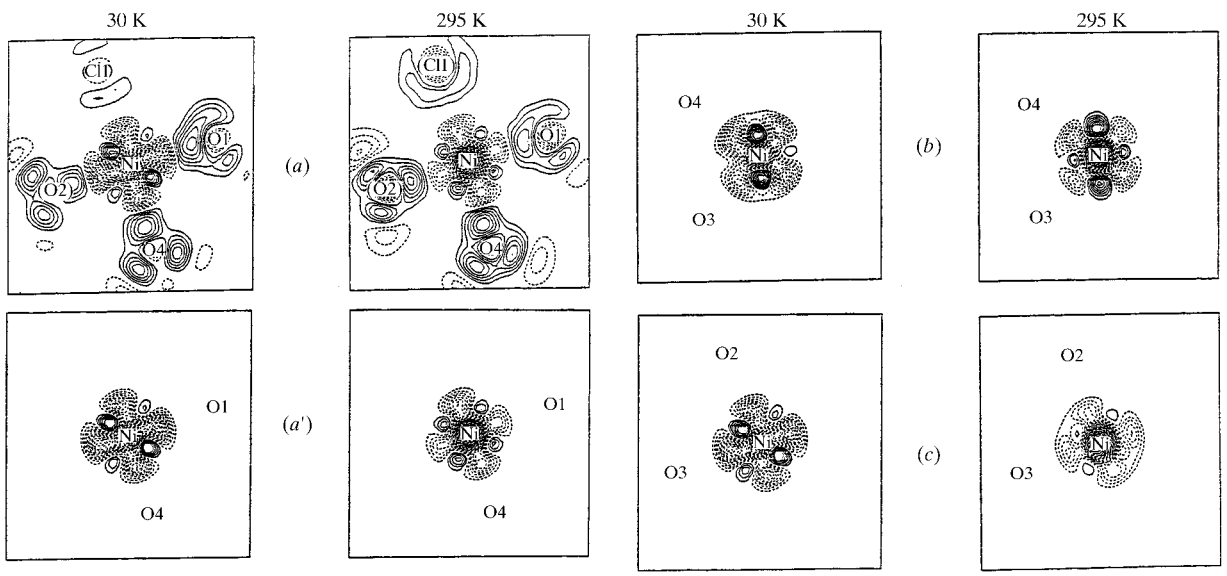

Fig. 4. Static deformation densities at 30 and 295 K in the plane defined by (*a*), (*a'*) Ni, O1 and O4; (*b*) Ni, O3 and O4; (*c*) Ni, O2 and O3. (*a*) All deformation functions included (total deformation maps). (*a'*), (*b*), (*c*) Only deformation functions centred on Ni included (partial deformation maps). Contours are drawn at intervals of 0.05 e $Å^{-3}$. Negative contours are dashed; the zero contour is omitted. Dimensions of maps: 6 × 6 Å.

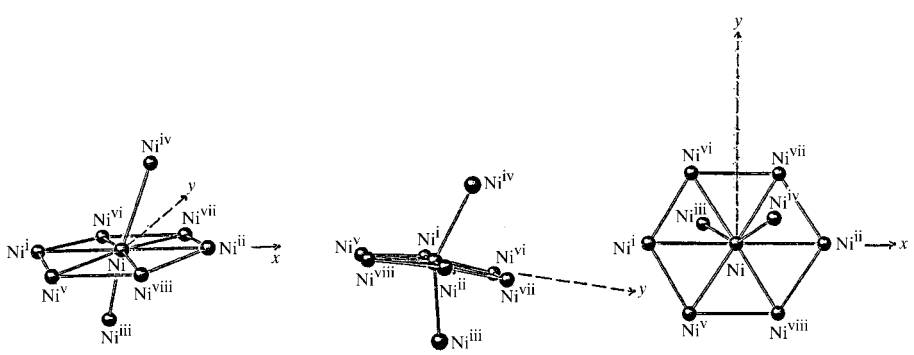

Fig. 5. The geometry of the nearest nickel neighbours of the nickel ion in the $NiCl_2.4H_2O$ structure (the *y* axes are not in the plane of the paper; *cf.* Table 4).

Table 4. *Geometry (Å, °) of the nearest nickel neighbours of the nickel ion in the $NiCl_2.4H_2O$ structure at 295 and 30 K*

	295 K	30 K
$Ni—Ni^{i}$	5.985 (3)	5.961 (2)
$Ni—Ni^{ii}$	5.985 (3)	5.961 (2)
$Ni—Ni^{iii}$	5.935 (3)	5.924 (2)
$Ni—Ni^{iv}$	5.935 (3)	5.924 (2)
$Ni—Ni^{v}$	5.593 (2)	5.585 (2)
$Ni—Ni^{vi}$	5.593 (2)	5.585 (2)
$Ni—Ni^{vii}$	5.477 (2)	5.461 (2)
$Ni—Ni^{viii}$	5.477 (2)	5.461 (2)
$Ni^{i}—Ni—Ni^{ii}$	180	180
$Ni^{i}—Ni—Ni^{iv}$	109.83 (3)	110.07 (5)
$Ni^{i}—Ni—Ni^{v}$	56.34 (2)	56.35 (2)
$Ni^{i}—Ni—Ni^{viii}$	121.78 (2)	121.66 (2)
$Ni^{i}—Ni—Ni^{vi}$	56.34 (2)	56.35 (2)
$Ni^{i}—Ni—Ni^{vii}$	121.78 (2)	121.66 (2)
$Ni^{i}—Ni—Ni^{iii}$	70.17 (3)	69.93 (5)
$Ni^{viii}—Ni—Ni^{vi}$	173.51 (1)	172.66 (1)
$Ni^{vii}—Ni—Ni^{v}$	173.51 (1)	172.66 (1)

Symmetry codes: (i) $x-1, y, z$; (ii) $x+1, y, z$; (iii) $x-\frac{1}{2}, -y+\frac{1}{2}, z-\frac{1}{2}$; (iv) $x+\frac{1}{2}, -y+\frac{1}{2}, z+\frac{1}{2}$; (v) $-x-\frac{1}{2}, y-\frac{1}{2}, -z+\frac{1}{2}$; (vi) $-x-\frac{1}{2}, y+\frac{1}{2}, -z+\frac{1}{2}$; (vii) $-x+\frac{1}{2}, y+\frac{1}{2}, -z+\frac{1}{2}$; (viii) $-x+\frac{1}{2}, y-\frac{1}{2}, -z+\frac{1}{2}$.

4.1.1. *The nickel(2+) ion*. The total and partial deformation densities at 30 and 295 K in one of the planes of the $Ni(H_2O)_4Cl_2$ complex are shown in Figs. 4(*a*) and (*a*′). Partial maps in two other planes are shown in Figs. 4(*b*) and (*c*). In all these sections the superposition effect is very small and the nickel densities in the total and partial maps are very similar. The deformation density of nickel shown in Figs. 4(*a*) and (*a*′), with excess deformation density in the diagonal directions and a deficiency in the ligand directions, is in qualitative agreement with that expected from crystal-field theory for an approximately octahedral coordination, but there are significant differences between the densities at 30 and 295 K in the planes illustrated in Figs. 4(*b*) and (*c*).

An extensive search in other planes around nickel has shown that the maximum features are actually not in the principal planes of the $Ni(H_2O)_4Cl_2$ complex, but in certain planes defined by the nearest neighbourhood of the Ni ion in a cation sublattice with the geometry shown in Fig. 5 and Table 4. This is illustrated by the partial maps in the three planes through nickel at 30 and 295 K in Fig. 6. The following scheme for specifying the planes of maximum deformation density around the metal ion in the crystal is proposed. In the nearly hexagonal surrounding of Ni in the network of Ni atoms, the plane normal to the line ($Ni—Ni^{i}$), which is the top edge of the 'partially' folded hexagon (Fig. 5), contains at least one direction with a maximum in the electron density (Fig. 6*a*). The remaining maxima lie in the plane perpendicular to this direction (Fig. 6*b*). The deformation density in the cross section through both directions (Figs. 6*a* and *b*) with a maximum in the electron density is shown in Fig. 6(*c*). The above scheme is only intended for a qualitative description, not for a detailed analysis of the experimental results.

The plane of maximum deformation density was observed according to the same scheme in $NiSO_4.7H_2O$ (Ptasiewicz-Bak *et al.*, 1997, Fig. 6) and $Na_2Ni(CN)_4.3H_2O$ (Ptasiewicz-Bak *et al.*, 1998, Fig. 5). In the first compound there were significant differences between the deformation density features at 295 and 30 K (Fig. 5), possibly related to small but significant differences in the Ni—Ni sublattice distances at the two temperatures; such differences are not found in the present compound.

The above illustrates that in discussing the electron densities around the nickel ion the interaction of the ion with the total crystal field should be taken into account,

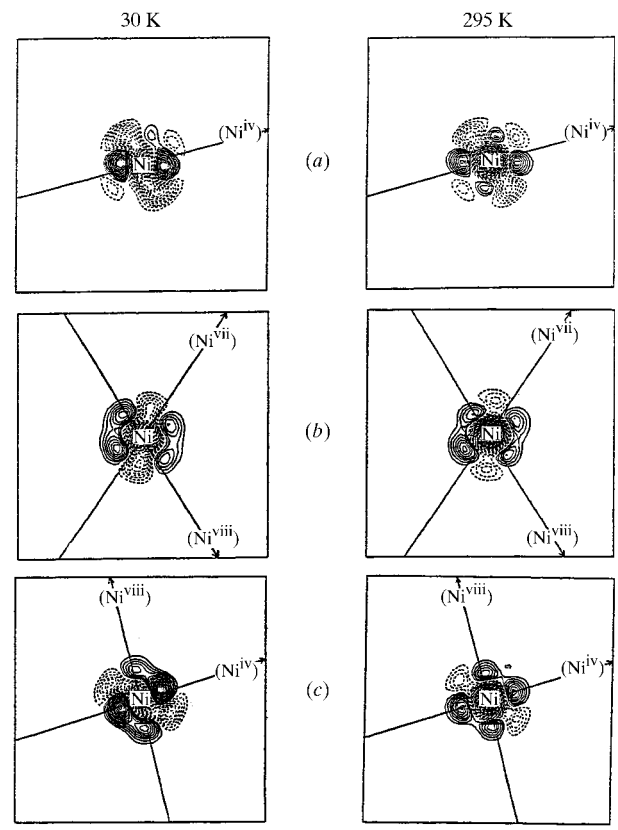

Fig. 6. Static partial deformation maps in three different planes through nickel, which do not involve the water ligands in the coordination octahedron, at 30 and 295 K. (*a*) Plane perpendicular to the $Ni—Ni^{i}$ line (Ni^{iv} is close to this plane). (*b*) Plane perpendicular to the $Ni—Ni^{iv}$ line (Ni^{vii} and Ni^{viii} are close to this plane). (*c*) Plane perpendicular to the $Ni—Ni^{vii}$ line (Ni^{iv} and Ni^{viii} are close to this plane). Ni^{i}, Ni^{iv}, Ni^{vii} and Ni^{viii} denote the equivalent positions described in Table 4 and illustrated in Fig. 5. Dimensions of maps: 6 × 6 Å. Contours are drawn at intervals of 0.05 e $Å^{-3}$. Negative contours are dashed; the zero contour is omitted.

not limiting it to the nearest ligands. Theoretical calculations, including the whole crystalline environment, are clearly desirable in this context.

4.1.2. *The water molecules*. The general features of the density in the O—H bond and the lone-pair region have been discussed in a previous paper (McIntyre *et al.*, 1990). The partial and total deformation densities in the present compound are illustrated for water (1) at 30 and 295 K in the water plane and perpendicular to this in Fig. 7. For comparison the corresponding maps for water (1), based on H-atom coordinates from the conventional X-ray refinement, are also shown in Fig. 7. The maps are very similar, which is not too surprising as the H-atom positions from X-rays (shifted out to 0.97 Å in the O—H directions) and from neutrons were rather similar. The corresponding maps for water (3) at 30 K are shown in Fig. 8(*a*). The superposition effect is quite noticeable in the lone-pair plane in the direction to nickel when comparing the total and partial maps.

Water (1) is tetrahedrally bonded to nickel and water (3) (*cf.* Fig. 3). As a consequence of this interaction there is a double peak in the lone-pair region, whereas there is just one 'banana-shaped' peak in the free water molecule according to theoretical *ab initio* calculations (Hermansson, 1984). The maps for water (2) (not shown), which is also tetrahedrally coordinated, are very similar. In contrast, water (3) is trigonally coordinated (*cf.* Fig. 3) and there is just one single peak in the lone-pair region (Fig. 8*a*), which is even more extended towards nickel than the peak in the free water molecule.

The situation for water (4) is more complicated. As described above (*cf.* §3), at 30 K atom H42 was found to be disordered and distributed over two positions, H421 and H422. The deformations densities involving all three alternative locations for H42, in planes corresponding to those for water (1) and water (3), are shown in Figs. 8(*b*), (*c*) and (*d*). The corresponding maps for water (4),

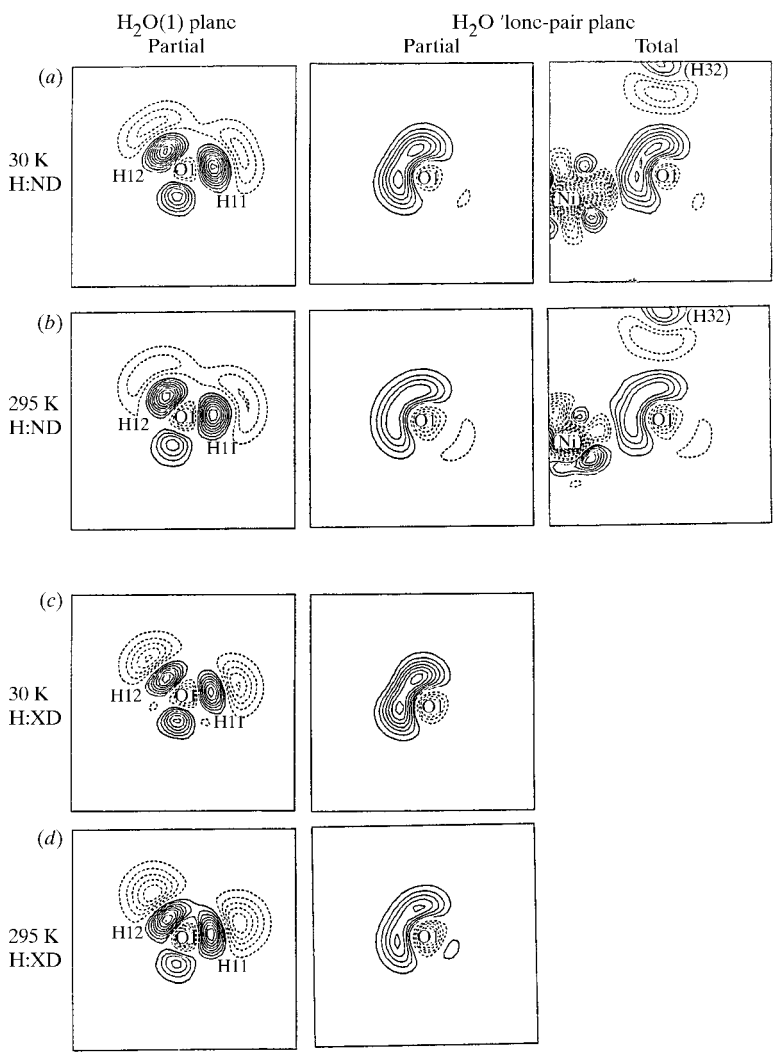

Fig. 7. Static partial and total deformation densities of the water molecule containing O1 at 30 and 295 K: in the water plane and perpendicular to this plane through the twofold axis (see text). Dimension of maps: 4.8 × 4.8 Å. H:ND = H-atom coordinates from neutrons. H:XD = H-atom coordinates from X-rays. Contours are drawn at intervals of 0.05 e $Å^{-3}$. Negative contours are dashed; the zero contour is omitted.

based on H-atom coordinates from the conventional X-ray refinement at 30 K, are very similar to the maps shown in Fig. 8(*b*).

It is most interesting to notice that the deformation density in the lone-pair plane of water (4) has a much more extended 'banana' shape (Figs. 8*b*, *c* and *d*) than in the other trigonally coordinated water (3) molecule (Fig. 8*a*). This might be due to influence from water (4^{vii}) [with $O4^{vii}$ at $(-x, -y, -z + 1)$], where $O4^{vii}$ is at a distance of only 2.893 (2) Å from O4 at 30 K compared with 3.012 (2) Å at 295 K. At 30 K the distance $O4\cdots H422^{vii}$ is 2.022 (29) Å and the angle $O4\cdots H422^{vii}—O4^{vii}$ is 157 (2)°. In comparison with hydrogen bonds at 295 K there is thus a new hydrogen bond at 30 K between two water molecules (with occupancies of 0.50): (O4, H41, H421) and (O4, H41, H422).

The agreement indices after the final deformation refinement are not that much better than those after the conventional refinement. If we had judged solely on the basis of these global indicators we might conclude that the modelled deformation charge distribution is insignificant. However, the model deformation maps clearly show features that we can accept on chemical and physical grounds, and which agree with those that we have observed in other similar transition-metal salt hydrates.

5. Concluding remarks

The same general conclusions can be drawn from this study as from our earlier experimental charge-density studies of nickel compounds, *i.e.* details of the deformation in and around water molecules can be extracted even in the presence of such strong X-ray scatterers as Ni, and the water molecules exhibit polarization that depends on their local environment.

The directions and features of maximum deformation density around nickel are almost the same at 30 and

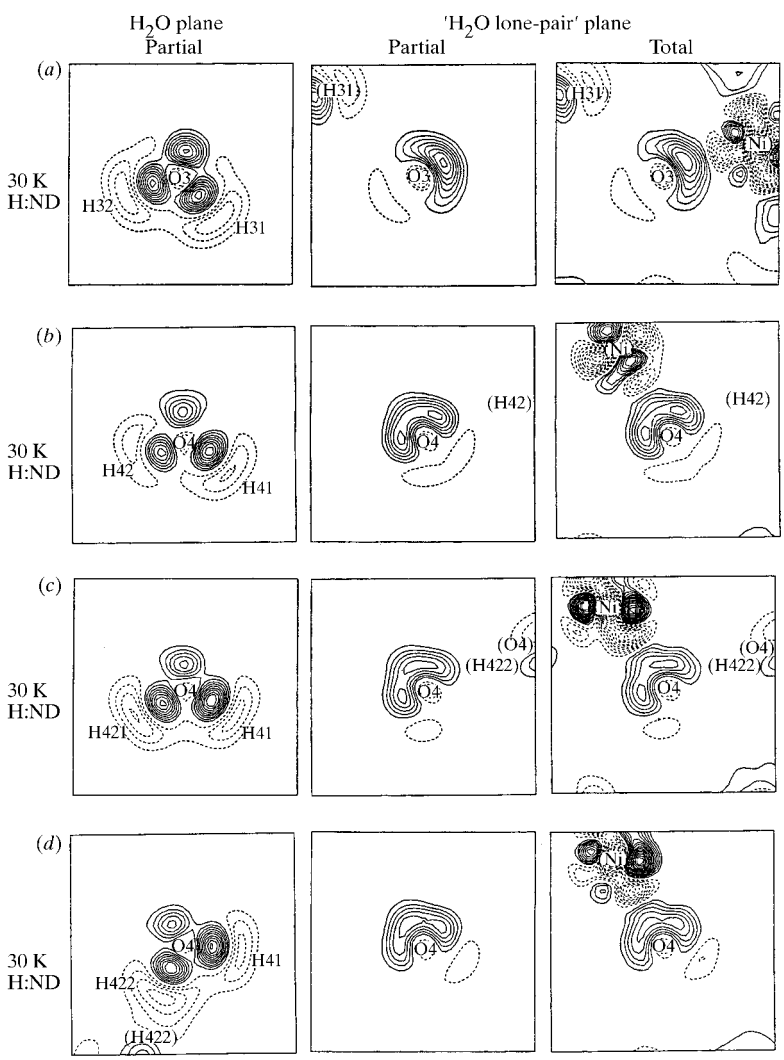

Fig. 8. Static deformation densities of water (3) and water (4) at 30 K in the water plane and perpendicular to this plane through the twofold axis. (*a*) Water O3. (*b*) Water (4) from refinement with the H42 average position (see text). (*c*), (*d*) Water (4) from refinement with H421 and H422 positions (see Table 2*d*). Dimension of maps: 4.8 × 4.8 Å. Contours are drawn at intervals of 0.05 e $Å^{-3}$. Negative contours are dashed; the zero contour is omitted.

295 K in the planes of maximum electron density, but not in the planes defined by ligands from the first coordination sphere. The deformation around Ni appears to be very sensitive to the influence of the whole crystalline environment.

The charge densities of water molecules with the same local coordination are largely transferable and, lacking neutron data, a reasonable picture of the deformation can be obtained using H-atom coordinates from the conventional refinement of the X-ray data by shifting H atoms along the O—H bond direction to the correct internuclear distance. This assumes though that there is no disorder or anharmonicity/libration in the H atoms. The present study illustrates that even poor-quality neutron data may be sufficient to identify disorder of the H atoms.

This work has been supported by a fellowship to HPB from the Royal Swedish Academy of Sciences through its Nobel Institute for Chemistry. We gratefully acknowledge the expert technical assistance of Hilding Karlsson in the collection of the X-ray data.

References

Becker, P. & Coppens, P. (1974). *Acta Cryst.* A**30**, 129–147.
Becker, P. & Coppens, P. (1975). *Acta Cryst.* A**31**, 417–425.
Harel, M. & Hirshfeld, F. L. (1975). *Acta Cryst.* B**31**, 162–172.
Hermansson, K. (1984). *Acta University Ups. Nova Acta Regiae Soc. Sci. Ups.* No. 744.
Hirshfeld, F. L. (1971). *Acta Cryst.* B**27**, 769–781.
Hirshfeld, F. L. (1977). *Isr. J. Chem.* **16**, 226–229.
Kellersohn, T., Delaplane, R. G., Olovsson, I. & McIntyre, G. J. (1993). *Acta Cryst.* B**49**, 179–192.
Lehmann, M. S., Kuhs, W., Allibon, J., Wilkinson, C. & McIntyre, G. J. (1989). *J. Appl. Cryst.* **22**, 562–568.
Lehmann, M. S. & Larsen, F. K. (1974). *Acta Cryst.* A**30**, 580–584.
Lundgren, J.-O. (1982). *Crystallographic Computer Programs.* Report UUIC-B13-4–05, Institute of Chemistry, University of Uppsala, Sweden.
McIntyre, G. J., Ptasiewicz-Bak, H. & Olovsson, I. (1990). *Acta Cryst.* B**46**, 27–39.
Olovsson, I., Ptasiewicz-Bak, H. & McIntyre, G. J. (1993). *Z. Naturforsch. Teil A*, **48**, 3–11.
Ptasiewicz-Bak, H., Olovsson, I. & McIntyre, G. J. (1993). *Acta Cryst.* B**49**, 192–201.
Ptasiewicz-Bak, H., Olovsson, I. & McIntyre, G. J. (1997). *Acta Cryst.* B**53**, 325–336.
Ptasiewicz-Bak, H., Olovsson, I. & McIntyre, G. J. (1998). *Acta Cryst.* B**54**, 600–612.
Samson, S., Goldish, E. & Dick, C. F. (1980). *J. Appl. Cryst.* **13**, 425–432.
Sears, V. F. (1986). *Methods of Experimental Physics*, Vol. 23A. *Neutron Scattering*, edited by K. Sköld & D. L. Price, pp. 521–550. Orlando: Academic Press.
Stewart, R. F., Davidson, E. R. & Simpson, W. T. (1965). *J. Chem. Phys.* **42**, 3175–3187.
Stroganov, E. V., Kozina, I. I., Andreev, S. N. & Koljadin, A. B. (1960). *Vestn. Leningr. University, Ser. Fiz. Khim.* **15**, 130–137.
Waizumi, K., Masuda, H. & Ohtaki, H. (1992). *Inorg. Chim. Acta*, **192**, 173–181.
Wilkinson, C., Khamis, H. W., Stansfield, R. F. D. & McIntyre, G. J. (1988). *J. Appl. Cryst.* **21**, 471–478.